

# Resolving neutrino mass hierarchy from supernova (anti)neutrino-nucleus reactions

D. Vale<sup>1</sup> and N. Paar<sup>1\*</sup>

<sup>1</sup>*Physics Department, Faculty of Science, University of Zagreb, Croatia*

(Dated: June 11, 2014)

We introduce a hybrid method to determine neutrino mass hierarchy by simultaneous measurements of detector responses induced by antineutrino and neutrino fluxes from accretion and cooling phase of type II supernova. The (anti)neutrino-nucleus cross sections for  $^{12}\text{C}$ ,  $^{16}\text{O}$ ,  $^{56}\text{Fe}$  and  $^{208}\text{Pb}$  are calculated in the framework of relativistic nuclear energy density functional and weak Hamiltonian, while the cross sections for inelastic scattering on free protons,  $p(\bar{\nu}_e, e^+)n$ , are obtained using heavy-baryon chiral perturbation theory. The simulations of (anti)neutrino fluxes emitted from a protoneutron star in a core-collapse supernova include collective and Mickheev-Smirnov-Wolfenstein effects inside star. The emission rates of elementary decay modes of daughter nuclei are calculated for normal and inverted neutrino mass hierarchy. It is shown that simultaneous use of (anti)neutrino detectors with different target material and time dependence of the signal allow to determine the neutrino mass hierarchy from the ratios of  $\nu_e/\bar{\nu}_e$  induced particle emissions. The hybrid method favors detectors with heavier target nuclei ( $^{208}\text{Pb}$ ) for the neutrino sector, while for antineutrinos the use of free protons and light nuclei ( $\text{H}_2\text{O}$  or  $-\text{CH}_2-$ ) represent appropriate choice.

PACS numbers: 21.10.Gv, 21.30.Fe, 21.60.Jz, 24.30.Cz

Over the past years a considerable progress has been achieved in constraining the mixing parameters in neutrino oscillation framework [1, 2], based on various experiments on atmospheric, solar, and terrestrial neutrinos [3]. It is now well established that neutrinos have nonvanishing rest masses and that the flavor states  $\nu_e$ ,  $\nu_\mu$ , and  $\nu_\tau$  are quantum mechanical mixtures of the vacuum mass eigenstates  $\nu_1$ ,  $\nu_2$ , and  $\nu_3$  [4]. However, currently existing data do not determine neutrino mass hierarchy, i.e., the sign of mass squared difference  $\Delta m_{31}^2 = m_3^2 - m_1^2$ . In the case of  $\Delta m_{31}^2 > 0$  one refers to normal mass hierarchy (NMH), while  $\Delta m_{31}^2 < 0$  corresponds to inverted mass hierarchy (IMH). Although a number of techniques has been proposed to resolve the neutrino mass hierarchy, to date this question still remains open and represents an important challenge in physics. Recent approaches to resolve the neutrino mass hierarchy include methods based on reactor neutrinos [5–7] different baseline experiments [8], Earth matter effects on supernova neutrino signal [9, 10], spectral swapping of supernova neutrino flavors [11], rise time of supernova  $\bar{\nu}_e$  light curve [12], analysis of meteoritic supernova material [13], and detection of atmospheric neutrinos in sea water or ice [14].

In this Letter we introduce a hybrid method to determine the neutrino mass hierarchy, based on type II supernova neutrino and antineutrino reactions with atomic nuclei, including,  $^{12}\text{C}$ ,  $^{16}\text{O}$ ,  $^{56}\text{Fe}$ ,  $^{208}\text{Pb}$ , and free protons. The aim is to explore how  $\nu_e$  and  $\bar{\nu}_e$  detectors, based on various nuclei as target material, can provide a source of information that is needed to determine the neutrino mass hierarchy. Since in the case of supernova event SN1987A mainly the  $\bar{\nu}_e$  sector of the response has been detected, the role of neutrinos and their relevance for understanding their underlying fundamental properties remain vastly unknown. While most of supernova detectors based on nucleon or nuclear targets are primarily

sensitive to antineutrinos, Helium and Lead Observatory (HALO) that was recently developed is sensitive to neutrinos through charged current (CC) interaction mainly with  $^{208}\text{Pb}$  [15]. For the purpose of the present study, microscopic theory framework based on relativistic nuclear energy density functional and weak Hamiltonian is employed in description of nuclear properties, neutrino induced excitations, and weak interaction transition matrix elements [16, 17]. In order to account for the  $\nu_e(\bar{\nu}_e)$ -induced events in detector, primary particle decay modes of daughter nuclei are described. In addition, to determine responses in water and mineral oil,  $\bar{\nu}_e$ -free proton cross sections are calculated in the framework introduced in Ref. [18], based on chiral perturbation theory.

Neutrino and antineutrino fluxes from the core-collapse supernova provide a powerful tool to probe various neutrino properties, as well as the dynamics of star explosion [19, 20]. They represent a kind of a fingerprint for the events occurring in stellar collapse and can be used for better understanding of neutrino flavor transformations in regions of high neutrino densities due to neutrino-neutrino interaction [19–24], and transitions occurring in matter resonance layers of star due to Mickheev-Smirnov-Wolfenstein (MSW) effect [25–27]. Region dominated by collective effects and two MSW resonant regions are spatially well separated, so probabilities of flavor transition can be calculated separately and multiplied. Both effects depend on neutrino mass hierarchy and change the shape of initial  $\nu_e(\bar{\nu}_e)$  spectra. Spectral splits and swaps in the  $\nu_e(\bar{\nu}_e)$  spectra caused by collective effects also depend on the flux ordering among different neutrino species, which are generally different in accretion and cooling supernova phase. Arrival of shock waves in the outer layers of a star can leave a mark on  $\nu_e(\bar{\nu}_e)$  spectra, even cause a non-adiabatic conversion, and multiple MSW effects [21].

For the purpose of this work, first we determine the

cross sections for the charged current  $\nu_e(\bar{\nu}_e)$  - nucleus reactions for the following target nuclei:  $^{12}\text{C}$ ,  $^{16}\text{O}$ ,  $^{56}\text{Fe}$  and  $^{208}\text{Pb}$ . The exclusive cross sections are described in the RNEDF framework [17, 28], by employing the density dependent effective interaction DD-ME2 [29]. Transition matrix elements for neutrino-induced reactions are calculated using the general formalism from Refs. [30, 31]. This method allows to determine in a consistent way the ground state properties of target nuclei and transitions induced by neutrinos. The exclusive cross sections are calculated as functions of excitation energy of initial nuclei, including all contributions from the initial ground state of even-even nucleus to the particular excited state, for all relevant multiplicities,  $J \leq 5$ , and both parities. Figure 1 shows the cross sections of  $\nu_e(\bar{\nu}_e)$  -  $^{56}\text{Fe}$  reactions with charge exchange, displayed as a function of the excitation energy in initial nucleus, for various multipoles,  $J^\pi = 0^\pm - 3^\pm$ . The cross section of  $\nu_e$  -  $^{56}\text{Fe}$  CC reactions is mainly determined by  $J^\pi = 0^+, 1^+$  transitions, while the contribution of  $J^\pi = 1^-, 2^-$  states is an order of magnitude smaller. Other multiplicities contribute only marginally. As shown in Fig. 1, in the case of  $\bar{\nu}_e$  -  $^{56}\text{Fe}$  reactions the cross section is dominated by  $J^\pi = 1^+$  transitions, with major contribution from the excited state at 4.5 MeV. In the limit of zero momentum transfer, the respective  $\text{GT}^\pm$  transitions result in reasonable agreement with respective experimental data [17, 32]. Energy threshold for CC reactions in  $^{56}\text{Fe}$  is relatively low for  $\nu_e$  (4.57 MeV) and  $\bar{\nu}_e$  (4.72 MeV). The  $\bar{\nu}_e$  -  $^{56}\text{Fe}$  cross sections are an order of magnitude smaller than in the neutrino case (Fig 1) due to the effect of Pauli blocking of neutron quasiparticle states.

Initial  $\nu_e(\bar{\nu}_e)$  spectra of the type II supernova can be described in the quasistationary approximation by the Fermi-Dirac or power law distribution [20–22]. One should note that initial neutrino fluxes are variable in time [33]. The fits to the available data from SN1987A have shown that average neutrino energy is relatively low, i.e.  $\sim 10$  MeV [21]. In the present work, the power law distribution is used to describe initial supernova neutrino spectra at neutrinospheres with fixed value of spectral parameter, i.e. 4.0 in the case of accretion neutrino flux and 3.0 during the whole cooling phase [36]. In numerical simulations of the neutrino accretion fluxes we fixed initial average energies of neutrinos to 12, 15 and 18 MeV for  $\nu_e$ ,  $\bar{\nu}_e$ , and non-electron species, respectively [22, 34, 35]. Certain deviations of previous values can be found in other supernova simulations [36]. In this work the best-fit values of neutrino oscillation parameters are used [37], except in region of collective oscillations where matter suppressed values of neutrino mixing are used instead [22]. For the initial accretion luminosities of (anti)neutrino species we take  $2.4 \times 10^{52}$  ergs in the case of  $\nu_e$ ,  $2.0 \times 10^{52}$  ergs for  $\bar{\nu}_e$ , and  $10^{52}$  ergs for all other (anti)neutrino species. In the supernova cooling phase neutrino luminosities are almost an order of magnitude

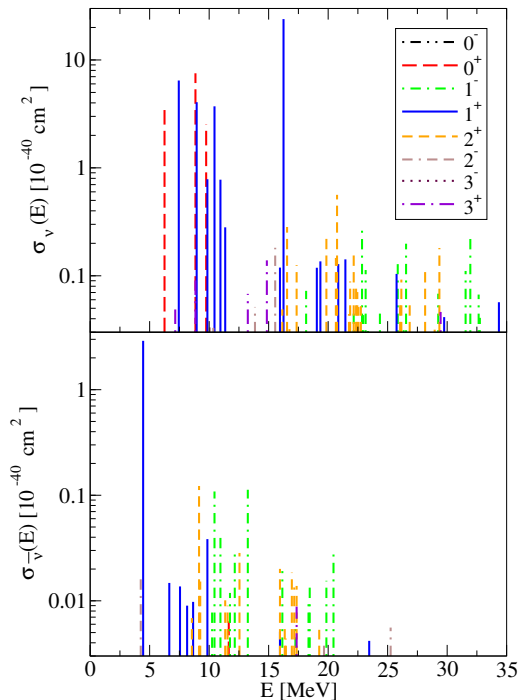


FIG. 1: Exclusive cross sections for  $\nu_e$  -  $^{56}\text{Fe}$  (upper panel) and  $\bar{\nu}_e$  -  $^{56}\text{Fe}$  (lower panel) reactions as a function of excitation energy in initial nuclei, including  $J = 0^\pm - 3^\pm$ .

smaller, i.e. the initial values we used are  $1.2 \times 10^{51}$  ergs for  $\nu_e(\bar{\nu}_e)$  and  $1.8 \times 10^{51}$  ergs for non-electron species, and the initial average energies of non-electron species are assumed 2 MeV higher than in the accretion phase [34]. The incoming (anti)neutrino fluxes are calculated including collective and MSW effects in the core-collapse star. Incoming  $\nu_e$  and  $\bar{\nu}_e$  fluxes of accretion and cooling supernova phase for normal (NMH) and inverted mass hierarchy (IMH) are shown in Fig. 2.

The calculated  $\nu_e(\bar{\nu}_e)$  - nucleus cross sections are used to determine the respective flux averaged values by employing  $\nu_e(\bar{\nu}_e)$  distributions shown in Fig. 2, and to evaluate the total number of detector events. In addition to  $\nu_e(\bar{\nu}_e)$  - nucleus cross sections, inelastic  $\bar{\nu}_e$  scattering on free protons is taken into account in mineral oil (alkanes based on  $-\text{CH}_2-$  group) and water ( $\text{H}_2\text{O}$ ). We employ the theory framework based on heavy-baryon chiral perturbation theory which also includes radiative corrections [18]. It is assumed that the detector efficiency is perfect, and it is turned directly to the incoming neutrino flux, thus eliminating the Earth effects on neutrino spectra. Four cases of target material are considered, mineral oil ( $\text{CH}_2$ ), water ( $\text{H}_2\text{O}$ ),  $^{56}\text{Fe}$ , and  $^{208}\text{Pb}$ . As a test case for type II supernova in our galaxy, an imaginary star 12000 l.y. away from the Earth is considered. We have calculated several neutrino induced decay channels, including  $\gamma$ , one-neutron (1n) and two-neutron (2n) emission, based on the limits given by the separation en-

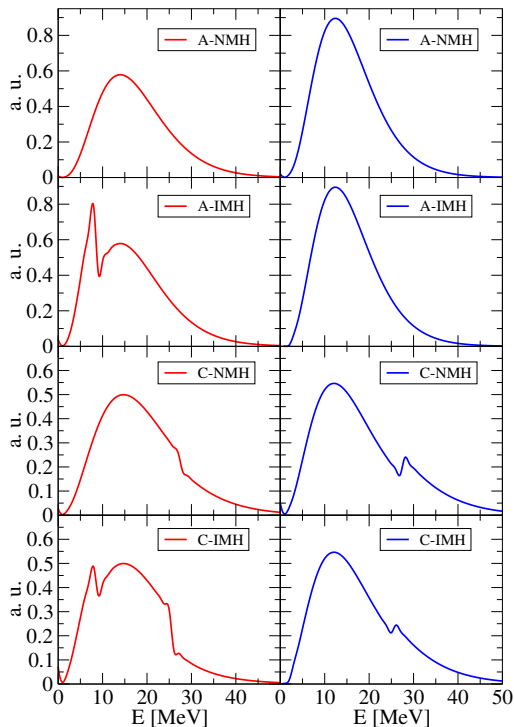


FIG. 2: Incoming  $\nu_e$  (left side) and  $\bar{\nu}_e$  fluxes (right side) for the accretion (A) and cooling (C) phase of type II supernovae as a function of neutrino energy for normal (NMH) and inverted neutrino mass hierarchy (IMH).

nergies  $S_{1n}$ ,  $S_{2n}$ ,  $S_{1p}$ , calculated from the implementation of the RNEDF in the relativistic Hartree-Bogoliubov model [29]. Table I shows the number of  $\nu_e(\bar{\nu}_e)$  - nucleus events (only dominant decay channels are shown) in 1 kt of target material based on  $^{56}\text{Fe}$  and  $^{208}\text{Pb}$ , and the number of emitted neutrons in case of  $\bar{\nu}_e - p$  reaction in mineral oil ( $\text{CH}_2$ ) and water ( $\text{H}_2\text{O}$ ). Calculations include incoming  $\nu_e(\bar{\nu}_e)$  fluxes of the accretion and cooling supernova phase, both for normal and inverted neutrino mass hierarchies. For the time duration of accretion and cooling supernova phase is taken 0.2 s and 10 s, respectively [35]. The results indicate a higher number of the events related to  $\nu_e(\bar{\nu}_e)$  in the case of NMH. Detector response of accretion  $\nu_e(\bar{\nu}_e)$  flux is characterized by the degeneracy in emission rates of  $\gamma$  rays, protons and neutrons for the entire set of target material and the best-fit values of neutrino oscillation parameters [37], i.e. it is invariant on the type of mass hierarchy. Similar result is obtained in simulations of supernova neutrino fluxes in case of  $^{208}\text{Pb}$  and large  $\theta_{13}$  mixing in [21].

The most pronounced response to CC interactions with neutrinos is obtained for  $^{208}\text{Pb}$ . It has large number of protons ( $Z = 82$ ), so the Coulomb effects enhance the phase space for emitted electrons [38], large neutron excess ( $N - Z = 44$ ) and relatively low threshold (2.88 MeV). The expected number of  $\gamma$  and proton events due to deexcitation of  $^{208}\text{Bi}$  is similar for both neutrino mass hierar-

TABLE I: Detector response for  $\nu_e(\bar{\nu}_e)$  - induced reactions in mineral oil ( $\text{CH}_2$ ), water ( $\text{H}_2\text{O}$ ),  $^{56}\text{Fe}$  and  $^{208}\text{Pb}$ , for the incoming (anti)neutrino fluxes of the accretion (A) and cooling supernova phase (C), both for normal (NMH) and inverted (IMH) neutrino mass hierarchies. Only dominant emission channels are shown, including  $\gamma$  rays, 1n and 2n emissions.

	NMH		IMH	
	$N(A)$	$N(C)$	$N(A)$	$N(C)$
$p(\bar{\nu}_e, e^-)n$ in $\text{CH}_2$				
1n	160	900	160	815
$p(\bar{\nu}_e, e^-)n$ in $\text{H}_2\text{O}$				
1n	125	700	125	635
$^{56}\text{Fe}(\nu_e, e^-)^{56}\text{Co}$				
$\gamma$	19	115	19	80
1n	17	137	17	80
$^{56}\text{Fe}(\bar{\nu}_e, e^+)^{56}\text{Mn}$				
$\gamma$	2	19	2	16
$^{208}\text{Pb}(\nu_e, e^-)^{208}\text{Bi}$				
$\gamma$	12	70	12	51
1n	84	533	84	350
2n	11	120	11	59

chies. Within the HALO detector [15], supernova neutrinos will be observed through neutron emissions from Pb target using  $^3\text{He}$  neutron detectors. For the supernova cooling phase, we obtain the flux averaged cross section related with 1n-emission from  $^{208}\text{Bi}$ :  $5.6 \times 10^{-40} \text{ cm}^2$  in the case of NMH, and  $3.8 \times 10^{-40} \text{ cm}^2$  in the case of IMH. However, significant contribution of 2n events due to relatively high 2n cross section rates is also obtained, i.e.,  $1.2 \times 10^{-40} \text{ cm}^2$  in the case of NMH and  $0.6 \times 10^{-40} \text{ cm}^2$  in the case of IMH. The resulting total number of emitted neutrons amounts  $\approx 880$  in the case of NMH, and  $\approx 575$  in the case of IMH, with the ratio of emitted neutrons  $N_n^{\text{NMH}}/N_n^{\text{IMH}} \approx 1.5$ . The sensitivity of 2n-emissions on the type of mass hierarchy is also obtained, i.e.,  $N_{2n}^{\text{NMH}}/N_{2n}^{\text{IMH}} \approx 2.0$ . The cross sections for  $\bar{\nu}_e$ - $^{208}\text{Pb}$  reactions are strongly suppressed (3 orders of magnitude) due to Pauli blocking of the neutron single-particle states.

The case of  $^{56}\text{Fe}$  target is characterized by somewhat weaker response to CC reactions with neutrinos (Tab. I), with almost half predicted events coming from  $^{56}\text{Co}$   $\gamma$  decay, while the other half mainly comes from 1n emission. The 1p and 2n emissions are severely reduced. However, due to smaller neutron excess ( $N - Z = 4$ ), detector based on  $^{56}\text{Fe}$  is also sensitive to antineutrino CC reactions with respective cross sections  $\sim 10^{-42} \text{ cm}^2$ , an order of magnitude smaller than for  $\nu_e$ - $^{56}\text{Fe}$  reaction. The predicted total cross section of neutrino induced reaction in  $^{56}\text{Fe}$  is  $\sim 10$  times smaller than for  $^{208}\text{Pb}$ . The total number of neutrons emitted from the detector (for  $\nu_e$  and  $\bar{\nu}_e$ ) based on  $^{56}\text{Fe}$  is  $\approx 165$  in the case of NMH and  $\approx 110$  in case of IMH, i.e., it is  $\approx 1.5$  times larger in the case of NMH.

In the case of mineral oil (water) of density  $0.85 \text{ g/cm}^3$  ( $1.0 \text{ g/cm}^3$  at  $4^\circ\text{C}$ ), where the target nuclei are  $^{12}\text{C}$  ( $^{16}\text{O}$ ), the predicted cross sections are of the order  $\sim 10^{-42} \text{ cm}^2$ , and due to  $N = Z = 6$  ( $N = Z = 8$ ) the difference in total number of primary events between neutrino and antineutrino CC reactions is smaller than for  $N > Z$  nuclei. Due to relatively high energy thresholds ( $\gtrsim 11 \text{ MeV}$ ) for both types of reactions in  $^{12}\text{C}$  ( $^{16}\text{O}$ ), at  $\nu_e$  ( $\bar{\nu}_e$ ) energies  $\lesssim 20 \text{ MeV}$  the responses are rather low. Actually, in the case of mineral oil (water)  $\bar{\nu}_e$  induce reactions mainly with free protons, resulting in 1060 (825) events in the case of NMH and 975 (760) events in the case of IMH, respectively (Tab. I). Dominance of  $\bar{\nu}_e - p$  reactions in mineral oil and water due to low energy threshold ( $1.8 \text{ MeV}$ ) and  $\sigma \sim 10^{-43} (E_\nu/\text{MeV})^2$  ensures an efficient coverage of  $\bar{\nu}_e$  spectra.

The results of the present analysis show that neither water or mineral oil can provide an evidence to determine neutrino mass hierarchy due to rather small difference of  $p(\bar{\nu}_e, e^+)n$  events for NMH and IMH fluxes (Tab. I). Therefore, we implement a hybrid approach, based on combination of detectors with different target materials to cover complementary parts of spectra in order to calculate relevant ratios of the events that are sensitive on the neutrino mass hierarchy. By focusing only on the cooling phase fluxes, the respective ratios of the neutron emissions for NMH and IMH in the case of combination of two detectors, 1 kt of water (free protons only) and 1 kt of  $^{208}\text{Pb}$  are:  $N_n^{\text{NMH}}(\text{H}_2\text{O})/N_n^{\text{NMH}}(\text{Pb}) = (0.91 \pm 0.05)$  and  $N_n^{\text{IMH}}(\text{H}_2\text{O})/N_n^{\text{IMH}}(\text{Pb}) = (1.36 \pm 0.08)$ . The statistical error of predicted events is estimated as  $\sqrt{N}$ . In addition, one can also use time-difference of accretion (A) and cooling (C) phase signal, and accretion degeneracy. Greater difference of ratios of emitted neutrons, i.e.  $N_C^{\text{NMH}}(\text{Pb})/N_A^{\text{NMH}}(\text{Pb}) = (7.3 \pm 0.8)$  and  $N_C^{\text{IMH}}(\text{Pb})/N_A^{\text{IMH}}(\text{Pb}) = (4.4 \pm 0.5)$ , once again confirms  $^{208}\text{Pb}$  as preferred target nucleus to cover the neutrino part of the spectra.

In conclusion, we have presented a hybrid approach to determine neutrino mass hierarchy from simultaneous measurements of supernova  $\nu_e$  and  $\bar{\nu}_e$  time difference in the events in detectors based on different types of target material. Through the use of supernova  $\nu_e$  ( $\bar{\nu}_e$ ) fluxes that include collective and MSW effects for the accretion and cooling phase, responses in mineral oil, water,  $^{56}\text{Fe}$  and  $^{208}\text{Pb}$  have been analyzed for both possible neutrino mass hierarchies. It is shown that the hybrid method, that combines antineutrino induced events in water or mineral oil, with neutrino induced emissions in heavier target nuclei such as  $^{208}\text{Pb}$ , provides a useful diagnostic tool to constrain the neutrino mass hierarchy. The number of emitted neutrons for the case of NMH is  $\approx 1.5$  larger than for IMH, both for  $^{208}\text{Pb}$  and  $^{56}\text{Fe}$  target nuclei. Since it is rather difficult to compare the absolute values of calculated particle emissions with the detector events, we have shown that the relative ratio of antineu-

trino and neutrino induced events in different detectors represent a quantity that could discriminate between different neutrino mass hierarchies. It is important to note that heavy nuclei are almost completely inert for CC reactions with antineutrinos due to strong Pauli blocking of neutron single particle states. Pure neutrino signal and large cross section establish  $^{208}\text{Pb}$  as probably the most important nuclear target for neutrino detection and reconstruction of the neutrino part of spectra. In case of the occurrence of the next galactic supernova, and taking into account current neutrino detector developments (e.g., HALO ( $^{208}\text{Pb}$ ) [15], Super-Kamiokande (water) [39], etc.) the hybrid method presented in this work would play an important role in constraining the neutrino mass hierarchy.

---

\* Electronic address: npaar@phy.hr

- [1] Z. Maki, M. Nakagawa, and S. Sakata, Prog. Theor. Phys. **28**, 870 (1962).
- [2] B. Pontecorvo, Zh. Eksp. Teor. Fiz. **53**, 1717 (1967) [Sov. Phys. JETP **26**, 984 (1968)].
- [3] M. C. Gonzalez-Garcia and M. Maltoni, Phys. Rep. **460**, 1 (2008).
- [4] A. Strumia and F. Vissani, arXiv:hep-ph/0606054 (2010).
- [5] S.T. Petcov, M. Piai, Phys. Lett. B **533**, 94 (2002).
- [6] Yu-Feng Li, Jun Cao, Yifang Wang, and Liang Zhan, Phys. Rev. D **88**, 013008 (2013).
- [7] F. Capozzi, E. Lisi, and A. Marrone, Phys. Rev. D **89**, 013001 (2014).
- [8] M. Ishitsuka, T. Kajita, H. Minakata, H. Nunokawa, Phys. Rev. D **72** 033003 (2005).
- [9] C. Lunardini and A. Yu Smirnov, J. Cosm. Astropart. Phys. **06**, 009 (2003).
- [10] B. Dasgupta, A. Dighe, A. Mirizzi, Phys. Rev. Lett. **101** 171801 (2008).
- [11] H. Duan, G. M. Fuller, J. Carlson, Y. Z. Qian, Phys. Rev. Lett. **99**, 241802 (2007).
- [12] P. D. Serpico, S. Chakraborty, T. Fischer et al., Phys. Rev. D **85**, 085031 (2012).
- [13] G. J. Mathews, T. Kajino, W. Aoki, W. Fujiya, and J. B. Pitts, Phys. Rev. D **85**, 105023 (2012).
- [14] W. Winter, Phys. Rev. D **88**, 013013 (2013).
- [15] C. Duba, F. Duncan, J. Farine, et al., J. Phys. Conf. Ser. **136**, 042077 (2008).
- [16] N. Paar, H. Tutman, T. Marketin, and T. Fischer, Phys. Rev. C **87**, 025801 (2013).
- [17] N. Paar, T. Suzuki, M. Honma, T. Marketin, and D. Vretenar, Phys. Rev. C **84**, 047305 (2011).
- [18] U. Raha, F. Myhrer, and K. Kubodera, Phys. Rev. C **85**, 045502 (2012).
- [19] Stuart Samuel, Phys. Rev. D **48**, 1462 (1993).
- [20] B. Dasgupta, A. Mirizzi, I. Tamborra, and R. Tomàs, Phys. Rev. D **81**, 093008 (2010).
- [21] D. Väänänen, C. Volpe, J. Cosm. Astropart. Phys. **10**, 019 (2011).
- [22] A. Mirizzi, and Ricad Tomas, Phys. Rev. D **84** 033013 (2011).

- [23] H. Duan, G. M. Fuller, and Y. Z. Qian, Phys. Rev. D **74**, 123004 (2006).
- [24] B. Dasgupta, and A. S. Dighe, Phys. Rev. D **77**, 113002 (2008).
- [25] L. Wolfenstein, Phys. Rev. D **17**, 2369 (1978).
- [26] A. S. Dighe, and A. Yu. Smirnov, Phys. Rev. D **62**, 033007 (2000).
- [27] A. Y. Smirnov, arXiv: 0305106v1 [hep-ph] (2003).
- [28] N. Paar, D. Vretenar, T. Marketin, P. Ring, Phys. Rev. C **77**, 024608 (2008).
- [29] G. A. Lalazissis, T. Nikšić, D. Vretenar, and P. Ring, Phys. Rev. C **71**, 024312 (2005).
- [30] J. S. O' Connel et al., Phys. Rev. C **6**, 719 (1972).
- [31] J. D. Walecka, Muon Physics, edited by V. M. Hughes & C. S. Wu (Academic Press, New York, 1975).
- [32] Y. F. Niu, N. Paar, D. Vretenar, and J. Meng, Phys. Rev. C **83**, 045807 (2011).
- [33] H.-Th. Janka, K. Langanke, A. Marek, and G. Martinez-Pinedo, Phys. Rep. **442**, 38 (2007).
- [34] S. Choubey, B. Dasgupta, A. Dighe, and A. Mirizzi, arXiv: 1008.0308 [hep-ph] (2010).
- [35] T. Fischer et al., Astr. Astrophys., **517A**, 80F (2010).
- [36] L. Hüdepohl, B. Muller, H. T. Janka, A. Marek, G. G. Raffelt, Phys. Rev. Lett. **104**, 251101 (2010).
- [37] G. L. Fogli et al., Phys. Rev. D **86**, 013012 (2012).
- [38] G. M. Fuller, W. C. Haxton, and G. C. McLaughlin, Phys. Rev. D **59**, 085005, (1999).
- [39] The Super-Kamiokande Collaboration, Nucl. Instr. Meth. A **737C** (2014).